

# A Novel Design of a Quadruped Robot for Home Safety

<sup>[1]</sup> Yu-Ping Liao, <sup>[2]</sup> Kai-Chi Lee, <sup>[3]</sup> Ming-Hao Lee, <sup>[4]</sup> Ting-Lin Lee, <sup>[5]</sup> Ruei-Chang Lu

<sup>[1][2][3][4]</sup> Department of Electrical Engineering, Chung Yuan Christian University, Taoyuan City, Taiwan (R.O.C.)

<sup>[5]</sup> Department of Electronics Engineering at National I-Lan University, Yilan City, Taiwan (R.O.C.)

Corresponding Author Email: <sup>[1]</sup> lyp@cycu.org.tw, <sup>[2]</sup> cage910715@gmail.com, <sup>[3]</sup> paul36534706@gmail.com, <sup>[4]</sup> 87558dany@gmail.com, <sup>[5]</sup> rclu@ems.niu.edu.tw

**Abstract**— As the population continues to age, the frequency of falls at home among older adults is increasing. Falls stand as the primary cause of injuries in this demographic. We proposed a novel design of a quadruped robot which combines autonomous cruising and AI-based accidental falls detection on a commercial available quadruped robot. The proposed system utilizes both human skeleton recognition and object recognition to identify accidental falls in home environments. The point clouds of a millimeter wave radar are processed in order to detection obstacles and navigation. If the predetermined conditions for an accident are met, an emergency notification is sent to the designated contacts.

**Index Terms**— Human skeleton recognition, falls detection, object recognition, millimeter wave (mmWave), quadruped robot.

## I. INTRODUCTION

As the global trend of aging continues to intensify, the safety and health of the elderly is becoming increasingly important. In Taiwan, in particular, the society is facing the challenge of ageing [1]. By 2030, It is expected that around 1 in 4 citizens (24.1%) will be aged 65 and above in Singapore [2]. This trend has brought about multiple issues, including the problem of childlessness, pressure on labor costs, and problems related to pet ownership, such as abandonment and difficulties in keeping pets.

The demographic changes triggered by the problem of childlessness may lead to a shortage of talent in the labor market, an increase in the burden of social welfare, and the questionable feasibility of an annuity system. The problem of manpower cost is exacerbated by the shortage of professional nursing manpower in the face of increasing demand for elderly care.

The problem of pet ownership involves an increase in pet abandonment, especially when the elderly is unable to take care of their pets, which may be abandoned. Pet ownership may also pose care, medical and socialization challenges, especially for the elderly with mobility problems. Recently, some bionic robots have been developed to mimic dog behavior [3][4]. Robotic pets require less maintenance compared to live pets [5].

To address these issues, a novel design of a quadruped robot for home safety is developed (Fig. 1). The system combines autonomous cruise, obstacle detection, and human fall recognition technologies to ensure the safety of the elderly in home. The proposed system integrates a mmWave radar module, a Raspberry Pi 4, a commercial available quadruped robot WAVEGO [6] and a camera to realize autonomous cruise and obstacle avoidance functions, and

recognize an accidental fall and notify family members. The novel design provides a powerful support needed by the future aging society to ensure the safety of the elderly at home.

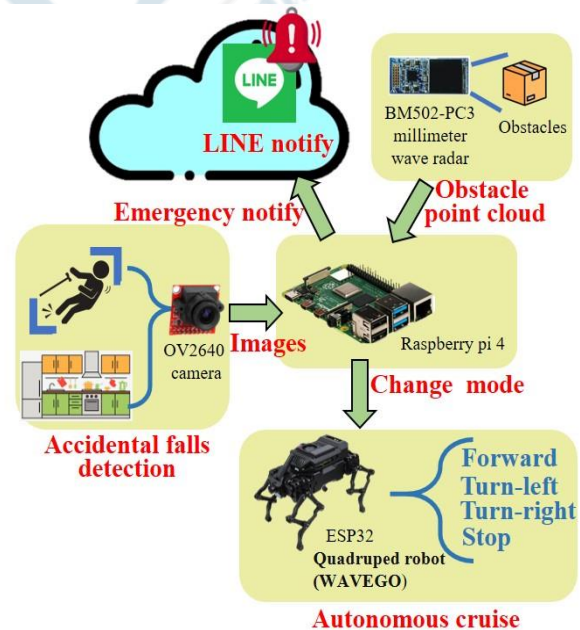


**Figure 1.** The proposed system.

The proposed work comprises two primary features. Firstly, the robot dog incorporates mmWave technology to detect obstacles and autonomously navigate around home during its cruise. It utilizes both human skeleton recognition and object recognition to identify and respond to accidental falls. Using the camera on the robot dog, photos are captured and sent to a human skeleton recognition system to determine whether the person is in a fallen state or not. If a fall is detected, the photos are then subjected to object recognition

to identify specific items in the current environment. Recognition of these specific items allows us to infer the current surroundings (e.g., identifying a pot suggests the environment is a kitchen). The system then assesses whether the current environment is a location where falling should not occur. If it is an inappropriate location for a lying, the system concludes that the person has experienced an accidental fall.

The organization of this paper is as follows: Section II outlines previous works in the field, while Section III presents the methodology employed in our system. Section IV presents the experimental results, followed by discussions in Section V. Finally, we conclude this paper.

## II. RELATED WORKS

The quadruped robot, a type of legged robot, excels in navigating challenging terrains, including steps, slopes, stairs, and rough landscapes [7]. These robots can be equipped with a variety of sensors, such as cameras, thermal cameras, lidars, laser range finders, and gas sensors. This sensor diversity makes them suitable for various applications such as inspection [8], delivery [9], rescue [10], and interaction with humans.

The basic function of a quadruped robot is obstacle detection. A robotic guide dog has designed to utilize two built-in RGB cameras to support effective navigation and obstacle avoidance [11]. The research [12] has developed an open-source low-cost quadruped robot covering aspects such as robot motion achieved through quadratic optimization and static stability of the center of gravity, a LiDAR-based simultaneous localization and mapping (SLAM) system, and path planning employing the A\* algorithm used a LiDAR-base. Due to the extensive data associated with image processing and lidar algorithms, the utilization of a graphics processing unit (GPU) is usually necessary for effective processing [13]. In contrast, millimeter wave radar is used to determine the location of objects without the need for complex algorithms [14]. Thus, the proposed system in this paper utilizes a mmWave radar to detect obstacles.

With the emergence of CNN- and DNN-based methods, human robot interaction has been significantly improved and has been applied in various scenarios. Nazarova et al. [15] introduced a deep neural network (DNN)-based interface for hand gesture recognition, enabling intelligent communication with a quadruped robot in 3D space. The gesture recognition interface enables operators to guide the quadruped robot using five distinct gestures and by altering the position of the palm in space. Li et al. [16] introduced an approach for single-person tracking and obstacle avoidance in quadruped robots. It involved gathering color and depth image data from a depth camera. The detection of individuals utilized the YOLOv3 deep learning neural network, providing position coordinate information for the quadruped robot to achieve human tracking. Sivacoumare et al. [17] introduced a cost-effective prototype created with a spider-type acrylic chassis, Raspberry Pi 4B, Pi camera module, and ESP32

microcontroller. The robot is furnished with various features, including an object detector, face detector and recognizer, speech recognizer, Chat-bot, and multiple Human-Machine Interface (HMI) methods. a cost-effective prototype created with a spider-type acrylic chassis, Raspberry Pi 4B, Pi camera module, and ESP32 microcontroller. The robot is furnished with various features, including an object detector, face detector and recognizer, speech recognizer, Chat-bot, and multiple Human-Machine Interface (HMI) methods. However, few studies have focused on detecting human falls with quadruped robots.

## III. METHODOLOGY

This section describes the proposed approach for the novel design of a quadruped robot for home safety. Fig. 2 shows the system flow. The quadruped robot incorporates millimeter-wave (mmWave) radar technology to detect obstacles during its cruise around home. It utilizes both human skeleton recognition and object recognition to identify and respond to accidental falls.

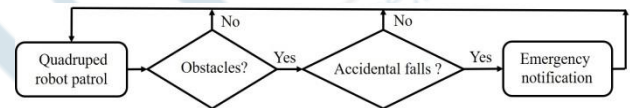


**Figure 2.** The flow of the proposed system.

### A. Obstacles detection with Millimeter-Wave Radar

Utilizing advancements in chip technology, Texas Instruments Incorporated (TI) has achieved successful development in millimeter-wave radar technology, which lowers the cost of millimeter-wave radar and makes it widely used in a wide range of applications [18]. With its compact structure, lower power consumption and higher resolution, the millimeter-wave radar has a different range of detection capabilities, namely short range, medium range and long range has a different range of detection capabilities, namely short range, medium range and long range.

A mmWave radar fundamentally estimates the distance, Doppler velocity, and angle of arrival of objects situated in its field of view, thus it can provide point cloud data of an object in front of it. Therefore, we can use millimeter wave radar to detect the direction and distance of obstacles [19]. The millimeter-wave radar used in this project is a millimeter-wave radar based on the Texas Instruments (TI) IWR6843AOP ASIC with frequency modulated continuous wave (FMCW) radar technology that operates in the 60 GHz to 64 GHz band, with FMCW up to 4 GHz, using three transmitter antennas and four receiver antennas, and using compact, low-power, multiple input multiple output (MIMO) radar waves. The FMCW radar waves are used to measure distance, velocity and angle parameters of a target [20].

Performing a coordinate transformation on the measured point cloud within a frame and store all computed coordinates in the same matrix, we found that within one frame, we can obtain about 150~300 points in a point cloud figure as shown

in Fig. 3. To ensure that smaller obstacles are not treated as noise, we perform three iterations of point cloud accumulation on the data.

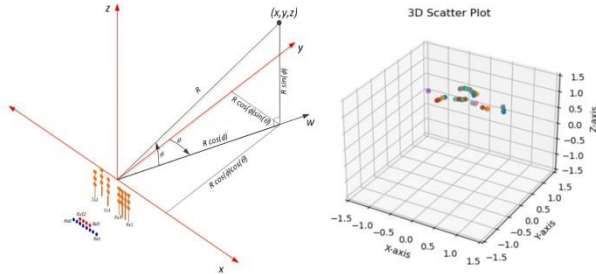


**Figure 3.** MmWave coordinate and measured point cloud

After accumulating point cloud data for three frames, we apply Density-based Spatial Clustering of Applications with Noise (DBSCAN) to the overlaid data [21][22]. This clustering analysis algorithm effectively and rapidly removes noise from the data. Among various clustering algorithms, DBSCAN has the advantage of handling large datasets, making it suitable for efficiently eliminating background noise in extensive point cloud data. The DBSCAN algorithm demonstrates effective clustering results in applications and serves as a typical representative of density-based algorithms. This algorithm is capable of identifying categories of arbitrary shapes within a dataset. DBSCAN requires users to set two global parameters before execution: neighborhood distance and threshold. The neighborhood distance defines the radius of the sample point's neighborhood range. The threshold is set by varying the minimum number of sample points marked as core points within the radius of the neighborhood range. It's important to note that both neighborhood distance and threshold are constants set before the program starts and remain unchanged thereafter. The DBSCAN algorithm is insensitive to noise points and can be applied to datasets containing noise points. It can identify and exclude noise points from clustering results. For each category in the clustering results, the density within the category is higher than at the category's edges, while the density of noise points is lower than at the edges. This algorithm utilizes density differences based on data distribution features to identify regions of different densities and labels the clustering results accordingly.

Applying the DBSCAN clustering analysis algorithm to the point cloud data collected by a mmWave radar is conducted to eliminate noise, as illustrated in the Fig. 4. Fig. 4(a) represents the raw point cloud data, where a significant amount of noise is observed. We utilize the DBSCAN clustering analysis algorithm to filter out noise from the original data, ultimately obtaining a signal with relatively low noise, as depicted in Fig. 4(b). Clustering, the process of grouping similar data objects into the same category, is commonly employed in data analysis. The division of a set of data objects into groups can be considered a form of data compression. One characteristic of clustering is its

unsupervised nature, distinguishing it from classification, which requires high costs in object modeling. Another feature of clustering is its adaptability to variations in data. Clustering can automatically discover and identify sparse and dense regions within a dataset.

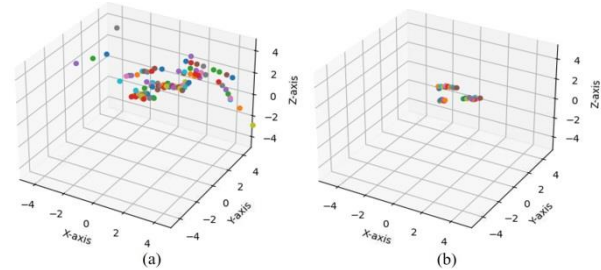


**Figure 4.** Point cloud (a) Before (b) After DBSCAN

### B. Human Skeleton Recognition

The human skeleton recognition utilized in this system is based on the pose detection with Mediapipe, which detects the skeletal pose by tracking 33 body landmark locations as shown in Fig. 5 [23]. The MediaPipe Pose Landmarker model lets users detect landmarks of human bodies in an image or video. You can use this task to identify key body locations, analyze posture, and categorize movements [24]. This task uses machine learning (ML) models that work with single images or video. The task outputs body pose landmarks in image coordinates with each point having its corresponding normalized data.

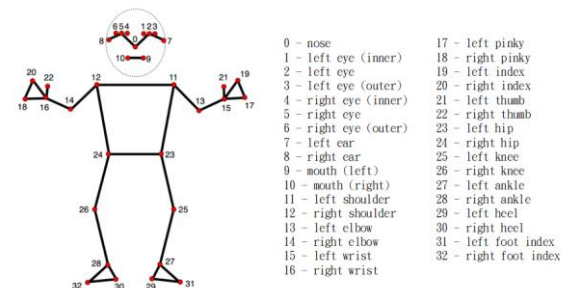


**Figure 5.** Mediapipe 33 body landmark locations [23]

The point data consists of three normalized parameters: x, y, z, and visibility. These correspond to the x-axis position, y-axis position, z-axis position, and visibility of the point in the camera's field of view, respectively. For x-axis data, 0 represents the far left side of the photo, 0.5 corresponds to the center point, and 1.0 represents the far right side. The y-axis data uses 0 for the bottom of the photo, 0.5 for the middle, and 1.0 for the top. The z-axis data represents depth, indicating the distance of the body from the camera. Visibility, a measure of how well each point on the body is visible, is expressed as a numerical value. Fig. 6 shows the y-axis data relative to the scale of the captured image with quadruped robot's field of view and the results of human skeleton recognition. Landmark point 11 indicates the position of the left shoulder, while point 12 corresponds to the location of the right shoulder.



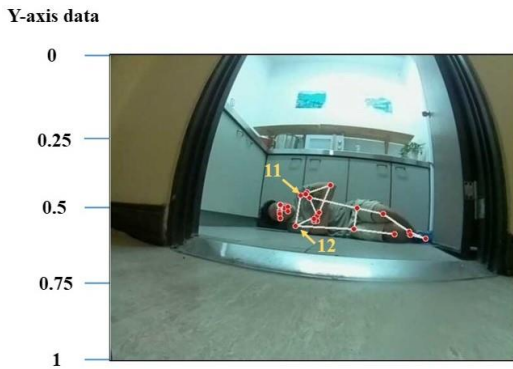


Figure 6. The captured image with the quadruped robot's field of view and the results of human skeleton recognition

Fig. 7 depicts an image with the quadruped robot's field of view that is 1 meter away from the quadruped robot. The normalized data for point 12 (right shoulder) and point 11 (left shoulder) is also depicted in Fig. 7. As far from a distance of 1 meter, the entire torso of a person can be captured in the image by the camera of the quadruped robot. If a person stands too close to the quadruped robot, the quadruped robot may not be able to see the person's head, and the landmarks will mark the points of head on both sides of the waist. In this study, we utilize the values associated with the left shoulder point 11 and right shoulder point 12 to identify whether an individual is in a fallen state or not.

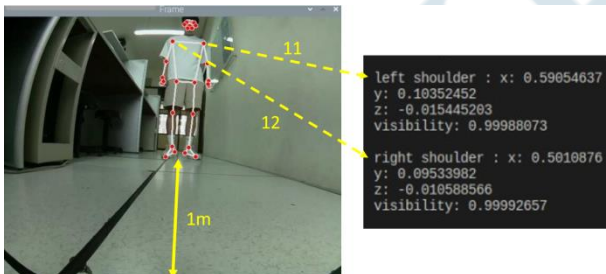


Figure 7. Skeleton recognition (standing) and shoulder data

### C. The Object Detection Model Trained on Roboflow

We utilize object recognition methods to infer the current environment because certain items are specific to particular environments. By using datasets consisting of these specific items and training a pre-trained object recognition system, we can identify these particular objects. In this way, we can deduce the current environment based on the recognition of specific items (e.g., detecting a pot implies being in the kitchen, detecting a toilet implies being in the bathroom). This approach enables us to determine the functionality of the current environment. We've employed the Roboflow cloud service to manage the photos and train the model for object recognition. Roboflow is a platform designed for computer vision projects, aiming to assist developers and teams in the seamless construction, training, and deployment of computer vision models [25]. Roboflow offers a range of tools and features, including the ability to download training sets, augment training data, and effectively handle image data for

machine learning model training. In the context of downloading training sets, the Roboflow universe hosts numerous datasets uploaded by other users, most of which are pre-annotated and ready for immediate use. Additionally, Roboflow provides proprietary AutoML models online. Models trained on the Roboflow platform have several advantages: convenience, fast training, low hardware load during application, and high accuracy. Leveraging this approach, our team operates two visual recognition tasks simultaneously on hardware. To achieve this, we make API requests to the server of the Roboflow, calling the models trained on their platform. The process involves sending the photos to be recognized, with the computation taking place in the cloud before transmitting the results back, resulting in reduced hardware load. The comparison of training time for the same task running on different platform is shown on Table 1.

Table 1. Training time comparison

Training environment	Time
Local computer (NVIDIA GeForce GTX 1650 Ti)	About 2 days
Google Colab	About 6 hours
Roboflow	About 2 hours

### D. Accidental Falls Detection System

Combining skeleton recognition and object detection, we have implemented a "Accidental Falls Detection System". The workflow of the system (Fig. 8) begins with skeleton recognition, checking if a person is in a fallen state. If the fall is detected, the system then utilizes the trained object recognition model to identify specific objects in the immediate environment, offering information about the surroundings. After understanding the environment, the system assesses whether the fallen state is in an inappropriate environment or not. If the result is yes, we can infer that an accident has occurred because the person is down in an unsuitable environment. Through the dual assessment of both recognition systems, we achieve the detection of individuals who have fallen due to an unexpected event.

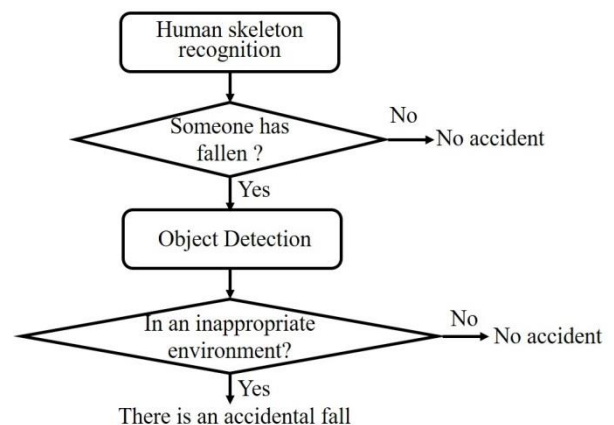


Figure 8. Accidental falls detection system flow

### E. Camera Calibration Using Chessboard

It is possible to rectify distorted images captured under wide-angle lenses after calibration. The "Zhang's Calibration Method" is a practical technique for camera calibration using a planar chessboard pattern [26]. Zhang's method employs a calibration board consisting of a grid of two-dimensional squares. The calibration process involves capturing images of the calibration board in various poses, extracting pixel coordinates of the detected corner points, calculating the initial intrinsic and extrinsic camera parameters using homography matrices, estimating distortion coefficients through nonlinear least squares, and finally optimizing the parameters using the maximum likelihood estimation method. The system optimizes using Zhang's chessboard calibration method to correct distorted images captured by wide-angle lenses, rectifying them to their intended straight-line appearance. In this research, the camera calibration was performed using a 10x7 standard checkerboard.

### F. Control of a Quadruped Robot WAVEGO

The WAVEGO is a commercial available quadruped robot. It uses the ESP32 as a controller for connecting rod inverse solving and gait generation. The quadruped robot can utilize a diagonal gait control known as the trot gait involving alternating support and swing legs [27][28]. The trot gait is a biomechanically efficient and stable walking pattern commonly observed in quadrupeds. It enhances the robot dog's maneuverability, providing a harmonious combination of support and movement. This gait is not only visually reminiscent of a dog's walk but also contributes to the overall stability and agility of the robot during locomotion. The gait emulation closely mimics the natural walking pattern of a dog. When leg2 and leg4 are in the swing phase, leg1 and leg3 maintain stable support to sustain the body of the robot dog as depicted in Fig. 9.

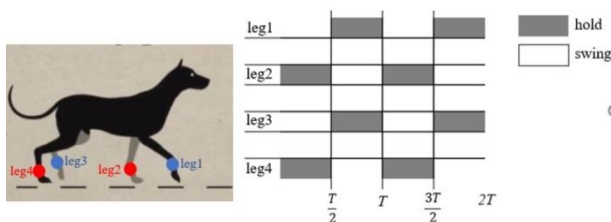


Figure 9. Common limb support sequences for dog trot gait

By incorporating diagonal gait control, WAVEGO robot dog achieves a dynamic and natural walking behavior, showcasing the versatility of its locomotion capabilities. This gait is essential for the robot's adaptability in navigating diverse terrains, making it a valuable feature for practical applications in real-world environments.

### G. Emergency Notification

The proposed system uses the Line notification API service of the instant messaging software Line to implement the function of instant notification of emergency contacts.

When you default a contact, you will be given a unique token for that specific contact. Through this token and Line notification API service URL, request the API service through HTTP Method post, and put in the emergency message that needs to be transmitted and the photo of the person who fell to complete the real-time notification.

## IV. EXPERIMENTAL RESULTS

In this novel design, we integrate a BM502-PC3 mmWave radar module [29] to a commercially available ESP32 controlled WAVEGO robot. We use a Raspberry Pi 3 to deal with the point cloud data from the mmWave radar. In addition, an OV2640 wide angle camera connected to a Raspberry Pi 4 is also combined in the WAVEGO for robot vision. The quadruped robot was decorated as a robot dog as shown in Fig. 10.

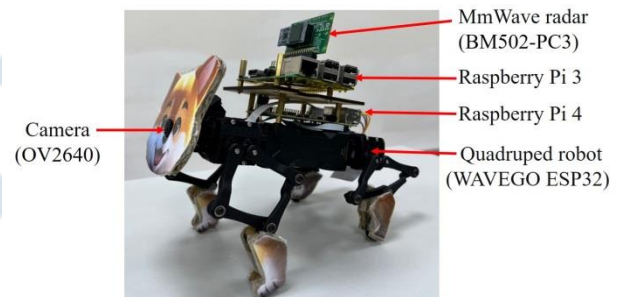


Figure 10. The implemented robot dog

### A. Object Detection

The proposed system uses mmWave radar to obtain point cloud data of obstacles. It was observed that when the millimeter-wave radar detects smaller objects, the number of points obtained is too few. This results in the subsequent clustering analysis process removing the point cloud data of smaller objects. To address this issue, experimental settings were adjusted to ensure that the millimeter-wave radar stores data for three consecutive frames before further proceeding. This ensures that the point cloud data of smaller objects is not excluded.

DBSCAN has two important parameters that need to be adjusted, namely eps radius and min\_samples minimum number of samples. Through experiments and adjustments of these two parameters, it was found that when the eps value is set too small, too much real obstacle point cloud data will be eliminated. In contrast, the noise cannot be effectively removed. When min\_samples is set too small, noise cannot be effectively eliminated. On the contrary, it will remove point cloud data of smaller obstacles. Table 2 illustrates the corresponding results of setting the two parameters of DBSCAN too large or too small. After multiple test, we have set the two parameters of DBSCAN to eps=0.5 and min\_samples=8.

**Table 2.** Comparison of setting parameters of DBSCAN

Setting	eps	min_samples
Too small	Identifying small roadblocks can be challenging.	It is difficult to distinguish between noise and signal.
Too large	It is difficult to distinguish between noise and signal.	Identifying small roadblocks can be challenging.

The following scenario is that there are two obstacles in front of the mmWave radar on the robot dog as illustrated in Fig 11(a), and Fig. 11(b) shows the distribution of acquired point cloud from the mmWave radar. In this system, we have set the number of accumulated frames to three and set the two parameters of DBSCAN to eps=0.5 and min\_samples=8.

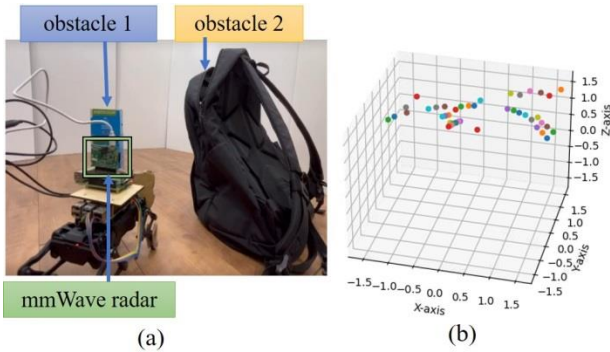


**Figure 11.** (a) Two obstacles in front of mmWave radar; (b) The acquired point cloud from the mmWave radar

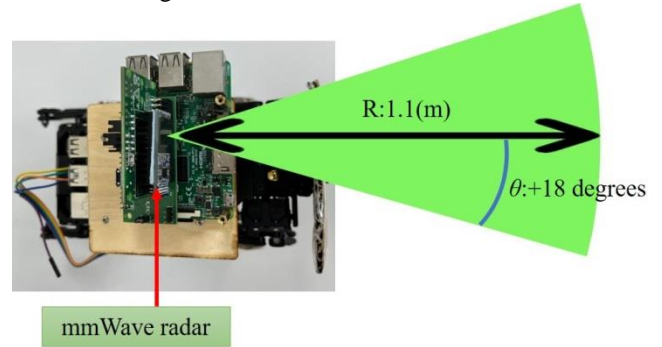
After removing noise from data, we extract the corresponding number by finding the minimum distance value and then determine the corresponding azimuth angle. This allows us to identify the direction of the nearest obstacle detected by the millimeter-wave radar, assisting the robot dog in obstacle avoidance responses. The original detection range of the millimeter-wave radar is a flat area of 6m\*6m. To enable the robot dog to navigate within confined spaces at home, we have defined effective detection range rules for the proposed system, as shown in the Table 3.

**Table 3.** Effective detection range for the proposed system

Obstacle Detection	Distance R (meter)	Azimuth $\theta$ (rad)
Obstacle detected	$0 \leq R < 1.1$	$-0.32 \leq \theta \leq 0.32$
No obstacles detected	$R \geq 1.1$	$\theta < -0.32$ or $\theta > 0.32$

We have set the effective detection range to be within 0 to 1.1 meters and within a fan-shaped region with angles ranging from -18 to +18 degrees as depicted in Fig. 12. In this figure, the green range we set is a region with a distance of 1.1 meters and an angle of 36 degrees. When an object appears within the green range, the robot dog is aware of an obstacle in front. Therefore, when an object is detected within

this range, the robot dog responds immediately and avoids the obstacle. On the contrary, when obstacles are outside this area, the robot dog does not consider them as obstacles and maintains a straight-line movement state.



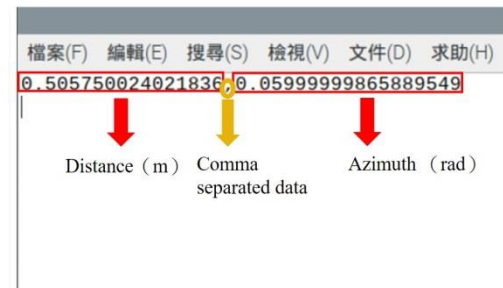
**Figure 12.** The obstacle detection range

Table 4 shows the corresponding results when the two parameters of the effective detection range are set too large or too small.

**Table 4.** Comparison of setting parameters of detection range

	Effective distance	Effective azimuth
Too small	Possible collisions during cruising.	Difficult to avoid obstacles.
Too large	Autonomous cruise failure.	Misjudges obstacles as non-collidable.

Since point cloud data from millimeter wave radar is processed in a Raspberry Pi 3 on the robot dog. The values of minimum distance and azimuth are stored in a specific text file on the Raspberry Pi 3. After each calculation of the minimum distance and corresponding azimuth angle, the text file content will be automatically overwritten. Fig. 13 illustrates the resultant text data stored in the Raspberry Pi 3.



**Figure 13.** The stored data of an obstacle

In addition, by establishing a Web server on the robot dog's Raspberry Pi 3 and creating an API for obstacle information, obstacle information can be accessed through the local area network.

### B. Human Skeleton Recognition

The robot dog uses an OV2640 wide angle camera connected to a Raspberry Pi 4 to capture image. The human skeleton recognition utilized in this system is based on the



pose detection with Mediapipe. By capturing the normalized y-axis data of point 12 (right shoulder) and point 11 (left shoulder), a test was conducted with the machine dog positioned 1 meter away from a person as depicted in Fig. 13.

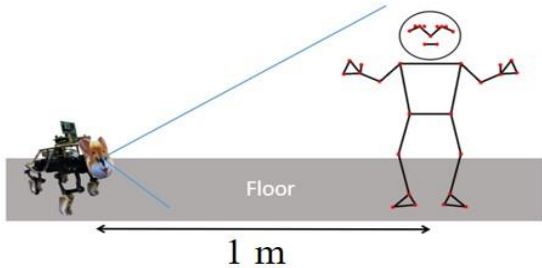


**Figure 14.** The robot dog tested 1 meter away from people

In the captured field of view, the highest point is represented by a value of 0, and the lowest point is represented by 1. Since the robot dog captures images from a low to high perspective, values above 0.6 indicate the floor. Through experimentation, it was observed that in a standing posture, the y-axis data for the shoulders is approximately 0.09, while in a squatting position, the data is around 0.3. Only when in a lying down or fallen posture do the shoulder positions become lower, with y-axis data exceeding 0.4 as shown in Table 7. Therefore, it is configured that when the y-axis data for points 11 and 12 is greater than 0.4, the person is considered to be in a fallen state.

**Table 5.** Example data of different human posture

Posture	Coordinates	Left shoulder	Right shoulder
Stand	X	0.59054	0.50108
	Y	0.10352	0.09533
Squat	X	0.59485	0.49069
	Y	0.30768	0.29989
Lying	X	0.56820	0.56831
	Y	0.53634	0.42345

Using a distance of 1 meter from the machine dog as a reference, experiments were conducted on shoulder point data in various postures. In a standing position, the data for both the left and right shoulders is around 0.1, and none exceeds 0.4, thus determining that the person is not fallen. In a squatting position, the data for both shoulders is around 0.2, with none exceeding 0.4, leading to the conclusion that the person is not fallen. In a side-lying position, the data for the left shoulder is 0.5, and the right shoulder's data is 0.4, with one data point exceeding 0.4, indicating a fallen state. Both lying on the back and lying on the stomach postures can be accurately recognized through skeleton detection, and at least one of the shoulder data points will exceed 0.4. Therefore, all lying postures can be recognized and determined as a fallen state.

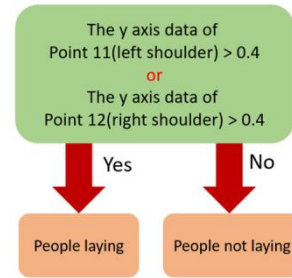


**Figure 15.** Human fall detection algorithm

**C. Object Detection Results**

We utilize object recognition methods to infer the current environment because certain items are specific to particular environments. By using datasets consisting of these specific items and training a pre-trained object recognition system, we can identify these particular objects. In this way, we can deduce the current environment based on the recognition of specific items. In the proposed system, when a pot is detected it means that the environment is a kitchen. We collected photos of pots from Roboflow universe and took some picture with the camera on the proposed robot dog.

**Table 6.** Image source

Source	Roboflow universe	Collected by the proposed robot dog	Total
Original Image quantity	1429	86	1515

We can easily generate augmented images with Roboflow. After undergoing rotations of positive and negative 12 degrees, adjustments in both vertical and horizontal angles, and saturation adjustments, the augmented photo set reached a total of 3637 images in the training dataset as shown in Fig. 16. This augmentation was done to adapt to objects at various heights, angles, and lighting conditions as depicted in Table 7.

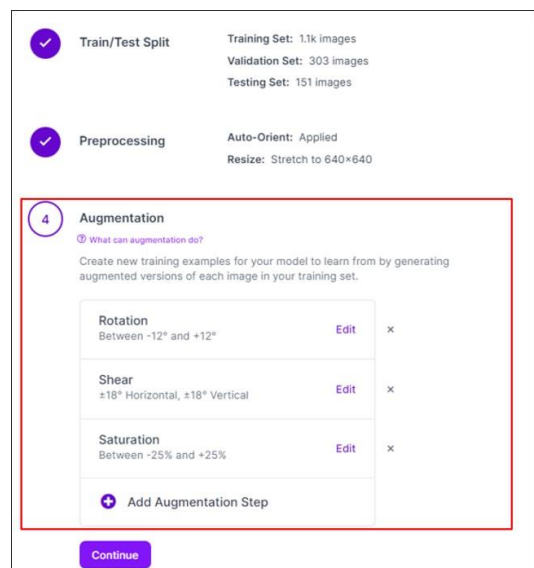


**Figure 16.** Augmentation on Roboflow

**Table 7.** Augmentation Setting

Type	Rotation	Shear	Saturation
Value	-12°~12°	±18°Horizontal, ±18°Vertical	-25%~25%

Then we started training and completed the training after 275 epoches. The trained model has mAP 96.8%, Precision 97.1% and Recall 94.2%. You can also see a significant decrease in the curves of Box Loss, Class Loss and Object Loss due to the number of training iterations. After completing the training of the model in Roboflow, it can be tested with various photos. Under normal conditions of object size, the model exhibits confidence levels of around eighty to ninety percent.

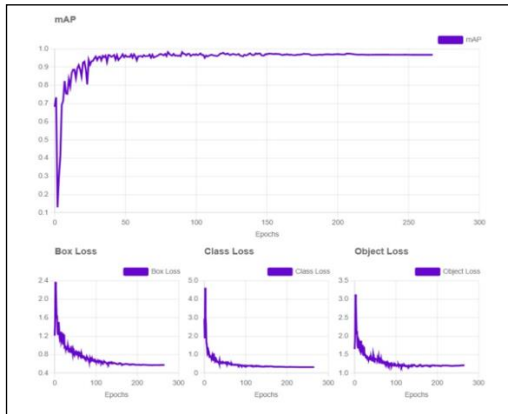


**Figure 17.** 3Model accuracy and various data curves

The model has been tested in pots, and the results are with a confidence level of over 80%. As shown in Fig. 18, the confidence level for the left pot is 88% and the confidence level for the right pot is 93%.



**Figure 18.** 4Model test results

**D. Accidental Detection and Emergency Notification**

The effective combination of skeleton recognition and object recognition forms an Intrusion Detection System. When a person is in a fallen state and located in an inappropriate environment (a pot is detected), the system recognizes this situation and implements a fall detection system for accidental events as shown in Fig. 19.

Older adults who fall commonly require emergency services. The recent advancements in Internet of Things (IoT) and machine learning has improved the autonomous assistance features a lot. Once a person is identified falls, object recognition is performed to assess the current environment. Based on the results of skeleton recognition and object recognition, if the predetermined conditions for an accident are met, an emergency notification is sent to the designated contacts with Line Notify as shown in Fig. 20.



**Figure 19.** Accidental fall detection results



**Figure 20.** Emergency nification through LINE Notify

**E. The System Workflow**

The proposed system employs AI models running on the Raspberry Pi 4 of the robot dog to perform tasks such as skeleton recognition and object recognition. By integrating the data of obstacles detected by mmWave, the Raspberry Pi 4 can transmit information to ESP32 of the WAVEGO via UART port and interrupt mechanisms of MCU. Subsequently, the WAVEGO can generate corresponding movements, such as stopping, turning left, turning right, and moving forward.

The autonomous obstacle avoidance component in this project involves a detailed workflow with the following steps as shown in Fig. 21:



Step 1: Millimeter-wave radar continuously gathers point cloud data in front of the robot dog, meticulously capturing the spatial arrangement of obstacles within its detection range.

Step 2: From the acquired obstacle point cloud data, the system identifies and retrieves the closest obstacle's precise distance and azimuth. This data provides critical information about the obstacle's proximity and angular position relative to the robot.

Step 3: Leveraging the azimuth information, the robot dog assesses the orientation of the obstacle, determining its specific location in the robot's field of view.

Step 4: The robot dog dynamically adjusts its direction, executing a precise maneuver to circumvent the obstacle effectively. This ensures the seamless integration of autonomous obstacle avoidance into the robot dog's navigation system.

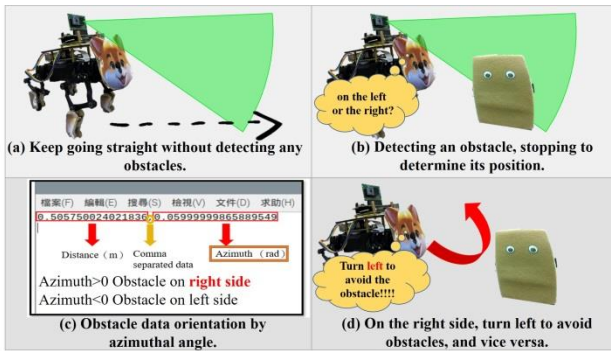


**Figure 21.** The workflow of obstacle avoidance

The workflow of the accidental detection component in this project comprises four detailed steps as shown in Fig. 22:

Step 1: Continuously collecting point cloud data in front of the robot dog through the utilization of millimeter-wave radar, enabling the precise the surrounding environment.

Step 2: Following the confirmation of the acquired data as valid point cloud information, the system proceeds to capture the current photo using an onboard camera. This photo is then subjected to skeleton recognition algorithms, accurately identifying human skeletal structures within the visual data.

Step 3: Simultaneously, advanced object recognition techniques are applied to discern and classify objects within the environment, contributing to a comprehensive understanding of the current surroundings.

Step 4: Leveraging the outcomes of both skeleton and object recognition, the system evaluates whether the conditions for an accidental event, as predefined, are met. If so, an immediate and automated emergency notification is dispatched to designated contacts, ensuring a swift response to potential incidents.

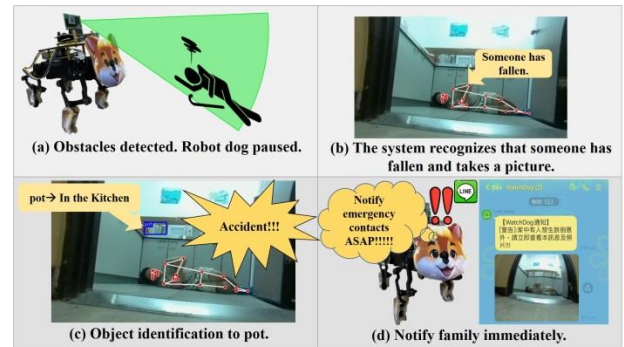


**Figure 22.** The workflow of the accidental detection

**V. DISCUSSION**

The proposed system utilizes an OV2640 wide-angle camera connected to a Raspberry Pi 4 to capture images. After calibration, distorted images captured with wide-angle lenses can be corrected. The curves in the photo are corrected back to their original straight shape, restoring the object to its practical appearance. When comparing pre-correction photos with post-correction photos of fallers, clear differences can be observed. Background objects, especially door frames, transform from their original curved state back to straight lines. Furthermore, employing checkerboard calibration can enhance the confidence of the trained model. As shown in Fig. 23, after camera calibration, the confidence of the small pot can be increased from 41% to 51%.

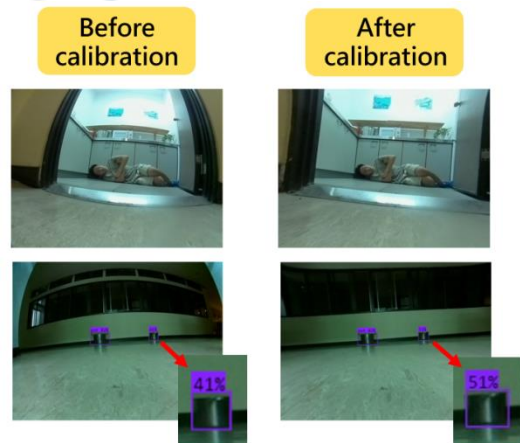


**Figure 23.** Comparison images before and after calibration

**VI. CONCLUSION**

In this paper, we propose a novel design of a quadruped robot that integrates autonomous patrolling, fall detection, object recognition, and obstacle detection technologies. We implemented and verified the design using millimeter-wave radar, a video camera, two Raspberry Pi boards, and a commercial quadruped robot. It uses human skeleton recognition and object recognition to identify accidental falls. The system can identify accidental falls in home and send an emergency notification to their families. This novel design

provides a strong guarantee for the aging society and ensures the safety of the elderly at home.

Current research projects on accident detection robot dogs are mainly focused on maintaining home safety. In terms of robot dog platforms, using larger and stronger robot dog carriers can smoothly navigate on various terrains and overcome terrain and load limitations. In terms of image recognition, by using various objects to upgrade the object recognition data set, the system can recognize various environments. This adaptability enables the accident detection system to be applied in various environments, such as long-term care centers or hospitals, overcoming the limitations of different scenarios.

## REFERENCES

- [1] Population Policy Data Collection. Dept. of Household Registration, Ministry of the Interior. Republic of China October 2022. [Online]. Available: <https://www.ris.gov.tw/app/en/676>
- [2] Population in Brief 2023, Singapore Department of Statistics, September 2023. [Online]. Available: <https://www.population.gov.sg/files/media-centre/publications/population-in-brief-2023.pdf>
- [3] H. Schellin et al., "Man's New Best Friend? Strengthening Human-Robot Dog Bonding by Enhancing the Doglikeness of Sony's Aibo," 2020 Systems and Information Engineering Design Symposium (SIEDS), Charlottesville, VA, USA, 2020, pp. 1-6, doi: 10.1109/SIEDS49339.2020.9106587.
- [4] A. Xiao, W. Tong, L. Yang, J. Zeng, Z. Li and K. Sreenath, "Robotic Guide Dog: Leading a Human with Leash-Guided Hybrid Physical Interaction," 2021 IEEE International Conference on Robotics and Automation (ICRA), Xi'an, China, 2021, pp. 11470-11476, doi: 10.1109/ICRA48506.2021.9561786.
- [5] M. K. Lee, J. Forlizzi, S. Kiesler, M. Cakmak and S. Srinivasa, "Predictability or adaptivity? Designing robot handoffs modeled from trained dogs and people," 2011 6th ACM/IEEE International Conference on Human-Robot Interaction (HRI), Lausanne, Switzerland, 2011, pp. 179-180.
- [6] WaveGo. [Online]. Available: <https://www.waveshare.com/wiki/WAVEGOhttps://www.waveshare.com/wiki/WAVEGO>
- [7] P. Biswal and P. K. Mohanty, "Development of quadruped walking robots: A review," Ain Shams Engineering Journal, vol. 12 no. 2, pp. 2017-2031, 2021. <https://doi.org/10.1016/j.asej.2020.11.005>
- [8] S. Yang et al., "Design of Mechanical and Hardware solutions for Quadruped robot chassis based on Substation inspection," 2023 IEEE 7th Information Technology and Mechatronics Engineering Conference (ITOEC), Chongqing, China, 2023, pp. 1826-1829, doi: 10.1109/ITOEC57671.2023.10292028.
- [9] M. Vikhe, N. Bothra, N. Malaviya, M. Kothari and R. Koshti, "Four Legged Parallel Manipulator for Autonomous Delivery Robot," 2023 International Conference on Device Intelligence, Computing and Communication Technologies, (DICCT), Dehradun, India, 2023, pp. 346-350, doi: 10.1109/DICCT56244.2023.10110234.
- [10] N. Li, J. Cao and Y. Huang, "Fabrication and testing of the rescue quadruped robot for post-disaster search and rescue operations," 2023 IEEE 3rd International Conference on Electronic Technology, Communication and Information (ICETCI), Changchun, China, 2023, pp. 723-729, doi: 10.1109/ICETCI57876.2023.10176723.
- [11] Y. Cao, N. Jin, Y. Wang, C. Ji and Y. Pan, "Bionic Robots as a New Alternative to Guided Dogs," 2023 9th International Conference on Virtual Reality (ICVR), Xianyang, China, 2023, pp. 261-267, doi: 10.1109/ICVR57957.2023.10169301.
- [12] F. García-Cárdenas, N. Soberón, O. E. Ramos and R. Canahuire, "Charlotte: Low-cost Open-source Semi-Autonomous Quadruped Robot," 2020 IEEE International Conference on Autonomous Robot Systems and Competitions (ICARSC), Ponta Delgada, Portugal, 2020, pp. 281-286, doi: 10.1109/ICARSC49921.2020.9096210.
- [13] Z. -Q. Zhao, P. Zheng, S. -T. Xu and X. Wu, "Object Detection With Deep Learning: A Review," in IEEE Transactions on Neural Networks and Learning Systems, vol. 30, no. 11, pp. 3212-3232, Nov. 2019, doi: 10.1109/TNNLS.2018.2876865.
- [14] N. Techaphangam and M. Wongsaisuwan, "Obstacle Avoidance using mmWave Radar Imaging System," 2020 17th International Conference on Electrical Engineering/Electronics, Computer, Telecommunications and Information Technology (ECTI-CON), Phuket, Thailand, 2020, pp. 466-469, doi: 10.1109/ECTI-CON49241.2020.9158273.
- [15] E. Nazarova, I. Babataev, N. Weerakkodi, A. Fedoseev and D. Tsetserukou, "HyperPalm: DNN-based hand gesture recognition interface for intelligent communication with quadruped robot in 3D space," 2022 IEEE International Conference on Systems, Man, and Cybernetics (SMC), Prague, Czech Republic, 2022, pp. 2043-2048, doi: 10.1109/SMC53654.2022.9945223.
- [16] Z. Li, B. Li, Q. Liang, W. Liu, L. Hou and X. Rong, "Research and Realization of Target Following and Autonomous Obstacle Avoidance Algorithm of Quadruped Robot," 2021 40th Chinese Control Conference (CCC), Shanghai, China, 2021, pp. 3984-3989, doi: 10.23919/CCC52363.2021.9550371.
- [17] A. Sivacoumare, S. M. S. S. Satheesh, T. Athul, M. V and T. Vinopra, "AI Quadruped Robot Assistant for the Visually Impaired," IECON 2021 – 47th Annual Conference of the IEEE Industrial Electronics Society, Toronto, ON, Canada, 2021, pp. 1-5, doi: 10.1109/IECON48115.2021.9589508.
- [18] A. Soumya, C. Krishna Mohan, L.R. Cenkramaddi, "Recent Advances in mmWave-Radar-Based Sensing, Its Applications, and Machine Learning Techniques: A Review," Sensors, 2023, vol. 23, no. 21, 8901, 2023. <https://doi.org/10.3390/s23218901>.
- [19] A. Pearce, J.A. Zhang, R. Xu, K. Wu, "Multi-Object Tracking with mmWave Radar: A Review," Electronics, vol. 12, no. 2, 308, 2023. <https://doi.org/10.3390/electronics12020308>

- [20] IWR6843AOP. [Online]. Available: <https://www.ti.com/product/IWR6843AOP>
- [21] J. Shen, X. Hao, Z. Liang, Y. Liu, W. Wang, and L. Shao, "Real-time superpixel segmentation by DBSCAN clustering algorithm," *IEEE Trans. Image Process.*, vol. 25, no. 12, pp. 5933–5942, Dec. 2016.
- [22] A. Karami and R. Johansson, "Choosing DBSCAN parameters automatically using differential evolution," *Int. J. Comput. Appl.*, vol. 91, no. 7, pp. 1–11, Apr. 2014.
- [23] Pose landmark detection guide. [Online]. Available: [https://developers.google.com/mediapipe/solutions/vision/pose\\_landmarker](https://developers.google.com/mediapipe/solutions/vision/pose_landmarker)  
[https://developers.google.com/mediapipe/solutions/vision/pose\\_landmarker](https://developers.google.com/mediapipe/solutions/vision/pose_landmarker)
- [24] A. Chittineni, Y. S. Kotagiri, M. Kolli, T. Kollipara, J. R. Modepalli and S. K. Namburi, "A Real-Time Virtual Yoga Assistant Using Machine Learning," 2023 3rd International Conference on Smart Data Intelligence (ICSMDI), Trichy, India, 2023, pp. 316-321, doi: 10.1109/ICSMDI57622.2023.00063.
- [25] S. G. E. Brucal, L. C. M. de Jesus, S. R. Peruda, L. A. Samaniego and E. D. Yong, "Development of Tomato Leaf Disease Detection using YoloV8 Model via RoboFlow 2.0," 2023 IEEE 12th Global Conference on Consumer Electronics (GCCE), Nara, Japan, 2023, pp. 692-694, doi: 10.1109/GCCE59613.2023.10315251.
- [26] Zhengyou Zhang, "Flexible camera calibration by viewing a plane from unknown orientations," *Proceedings of the Seventh IEEE International Conference on Computer Vision, Kerkyra, Greece, 1999*, pp. 666-673 vol.1, doi: 10.1109/ICCV.1999.791289.
- [27] W. Fuping and Z. Zhengjun, "Research on Inverse Kinematics of Robot Based on Motion Controller," 2018 IEEE International Conference of Intelligent Robotic and Control Engineering (IRCE), Lanzhou, China, 2018, pp. 34-37, doi: 10.1109/<https://ieeexplore.ieee.org/stamp/stamp.jsp?tp=&arnumber=8492954&isnumber=8492914>
- [28] Y. Xin, B. Liu, X. Rong, B. Li and H. Wang, "Research on smooth trot-to-walk gait transition algorithm for quadruped robot," 2017 Chinese Automation Congress (CAC), Jinan, China, 2017, pp. 5967-5971, doi: 10.1109/<https://ieeexplore.ieee.org/stamp/stamp.jsp?tp=&arnumber=8243851&isnumber=8242722>
- [29] BM502-PC3. [Online]. Available: [http://www.joybien.com/product/P\\_mmwave\(BM502\\_PC3\).html](http://www.joybien.com/product/P_mmwave(BM502_PC3).html)